Available online at www.sciencedirect.com

Cement and Concrete Research 36 (2006) 1231 – 1239

Relating the molecular structure of comb-type superplasticizers to the compression rheology of MgO suspensions

Ane M. Kjeldsen [a], Robert J. Flatt [b], Lennart Bergström [c,*]

[a] *Department of Civil Engineering, Technical University of Denmark, Building 118, Brovej, Kgs Lyngby DK-2800, Denmark*
[b] *Sika Technology AG, Tüffenwies 16, Postfach, CH-8048 Zurich, Switzerland*
[c] *Materials Chemistry Research Group, Department of Physical, Inorganic and Structural Chemistry, Arrhenius Laboratory, Stockholm University, SE-106 91, Stockholm, Sweden*

Received 20 September 2005; accepted 22 March 2006

Abstract

We have investigated the effect of superplasticizers on the rheological properties of concentrated MgO suspensions. The comb-type anionic polymers with grafted polyethylene oxide chains adsorb onto the MgO surface and infer a steric repulsion where the range scales with the length of the PEO side chains. Consolidation experiments, where the volume fraction gradient of particle networks has been determined in response to a centrifugal force field, offer a simple, yet accurate, way of investigating flocculated, partly stabilized and stable suspensions under compression. The compression rheology behaviour could be related to the estimated thickness of the adsorbed superplasticizers and a scaling analysis was used to quantitatively assess the importance of the length of the grafted PEO-chains on the magnitude of the inter-particle bond strength.

Keywords: Rheology; Superplasticizers; Cement; Suspensions; Polymers

1. Introduction

Superplasticizers are able to reduce the porosity of the hardened concrete by allowing the fresh material to become workable with less water. This greatly enhances the durability and also makes it possible to substitute substantial volumes of cement with industrial waste materials, e.g. slag and fly ash [1]. The first generations of superplasticizers, e.g. sulphonated naphthalene formaldehyde (SNF) and modified lignosulphonates (LS), resulted in significant improvements of the properties of fresh concrete and they are still widely used. Increasing demands on workability, high strength and enhanced durability spurred the development of new types of synthetic superplasticizers with improved performance [2,3]. These new generation superplasticizers are comb-type copolymers with an anionic backbone, commonly having carboxylic and/or sulphonate groups that can render the polymer a negative charge, and un-charged poly(ethylene oxide (PEO))-based chains of variable length grafted onto the anionic backbone at regular intervals.

Numerous studies have investigated the mode of action of superplasticizers. Superplasticizers adsorb at the solid–liquid interface, and can impart a repulsive inter-particle force of electrostatic or steric origin that reduces or eliminates the adhesion between particles at close proximity. Their relative importance of the double-layer and the polymer-induced contributions in reducing the degree of flocculation has been an issue of several studies. The high ionic strength and the relatively low surface charge densities in cementitious systems suggest that the steric repulsion should be dominating, in particular for the new comb-type copolymers [4–6]. However, there are also studies suggesting that non-adsorbed polymers may play an important role, either through depletion interactions [7] or nucleation inhibition [8].

There is a lack of quantitative experimental studies, relating the rheological properties to the polymer architecture, that corroborate the theoretical predictions based on calculations on inter-particle forces [5,9] on cementitious systems. Systematic studies have been restricted by a limited access to a range of

---

* Corresponding author. Tel.: +46 8 162368.
E-mail address: lennartb@inorg.su.se (L. Bergström).

0008-8846/$ - see front matter © 2006 Elsevier Ltd. All rights reserved.
doi:10.1016/j.cemconres.2006.03.019

well-characterised polymers and also faced problems with quantification that are related to the very low yield stresses that the comb-type superplasticizers usually infer at full surface coverage. Hence, previous work has mainly reflected how the adsorbed amount at sub-monolayer coverage is related to the flow and rheology. Yamada and Hanehara [10] showed that competitive adsorption of sulfates decreases adsorption and thereby flow. Schober and Mäder [11] found that the spread of cement paste dispersed with various comb-type polymers varied linearly with the adsorbed amount regardless of the length of the grafted side chains.

This study aims for a more fundamental understanding of the stabilisation mechanism of comb-type superplasticizers. We have related the rheological behaviour to the conformation of the adsorbed superplasticizers. Inert suspensions of MgO in an ionic solution, representing that of an ordinary Portland cement paste (OPC, measured on a paste with $w/c = 0.5$ after 30 min), were used as a model system for cement. We have used a range of comb-type superplasticizers with a systematic variation in the length of the grafted polyethylene oxide side chains. The study was performed by centrifugal consolidation, also known as compressive rheology, which exploits rather than suffers from the tendency of a dispersed or weakly flocculated suspension to sediment. The conformations of the adsorbed polymers were estimated from scaling arguments [12,13] and the layer thickness and the associated inter-particle bond strength could be related to the density of the consolidated particle networks.

2. Materials and methods

2.1. Materials

2.1.1. MgO

Magnesium oxide (MgO) was used as a relatively inert model system for cement [14]. Model systems should have a pH sufficiently high to allow full ionisation of the superplasticizer ($\text{pH} > 12$). Furthermore, the average zeta potential should be close to zero and the system should be chemically stable in the presence of divalent cations. Previous work has shown that MgO has a surface charge similar to that of cement, with a zeta potential close to zero at pH 12.5 [15]. However, recent work has shown that MgO is not completely inert at pH 12 [14,16], and that an initial hydration to $Mg(OH)_2$ takes place. This hydration reaction essentially stops after 30 min and offers stable conditions for about 3.5 h, before further conversion takes place, as determined by specific surface area measurements previously reported [16] and given in Table 1. The dead burned MgO powder used in the consolidation experiments had a density of 3.58 g/cm^3 and was from Martin Marietta Magnesia Specialties Inc. (Type MagChem P98, Baltimore, U.S.A.). This powder was air classified to obtain a powder with a particle size finer than 10 μm. All the experimental studies were performed within the 3 h stable period after the powder has been mixed with water.

2.1.2. Electrolyte

We have chosen to work with an ionic solution that mimics the aqueous phase of the cement suspensions. Mixing cement suspensions with a water/cement ratio (w/c) of 0.5 during 30 min results in a supernatant that is supersaturated with respect to syngenite ($K_2Ca(SO_4)_2 \cdot H_2O$), which can result in precipitation. Dr. Yves Houst (EPFL) proposed to replace the potassium ions by sodium, which minimizes the risk of precipitation without affecting the ionic strength of the solution (unpublished work). In what follows we refer to this solution as YS (Yves' Solution). The YS is composed of 2.07 g/L of $CaSO_4 \cdot 2H_2O$, 12.5 g/L of Na_2SO_4 and 2.92 g/L of NaOH and has an ionic strength of 0.415 M, and a pH of 12.8.

Table 1
Properties of MgO powder after exposure to water at pH 12 (from [16])

Powders	SSA* (m^2/g) as-received powder	SSA* after 30 min (m^2/g)	SSA* after 60 min (m^2/g)	Median volume diameter (μm)
MgO P98-C	2.51 ± 0.01	7.53 ± 0.03	7.55 ± 0.08	2.90 ± 0.5

SSA: specific surface area.

2.1.3. Superplasticizers

We have used six different comb-type superplasticizers (noted PC 1–4 and A–B) in the study. All the polymers are composed of a polymethacrylic (PMA) backbone and grafted side chains of polyethylene glycol (PEG) and the length of the backbone and the grafted side chains have been systematically varied. The polymers PC 1–4 were used in an EC-project called “Design and function of novel polymeric admixtures for more durable high performance concrete” and some details of these polymers have been published [11,16–19]. The polymers A and B were synthesised specially for this study.

Schematic drawings of the polymers are shown in Fig. 1. Mass average molecular weights determined by GPC are given in Table 2 for the polymers. Side chain lengths are nominal values provided by the supplier. The backbone length is back-calculated from grafting degree and polymer molecular mass.

Adsorption data obtained by Perche [16] by solution depletion on suspensions of MgO is reported in the same table. The experimental procedure for those measurements is described in [17]. All polymers were ultrafiltrated to eliminate unreacted components or oligomers.

2.2. Experimental procedures

2.2.1. Suspension preparation and centrifugation

Concentrated MgO suspensions at solids concentration of 20 vol.% were prepared by mixing the MgO powder with the electrolyte solution YS. The MgO suspension was ultrasonicated in an ultrasonic bath for 5 min and then left with magnetic stirring for 30 min until the initial hydrolysis period had been completed. The polymers were added and the suspension was equilibrated for 30 min under magnetic stirring. We added an amount of polymer of 6 mg of polymer/g of the MgO powder, which ensures that the MgO surface is saturated by the polymer. One set of experiments was also performed at sub-monolayer

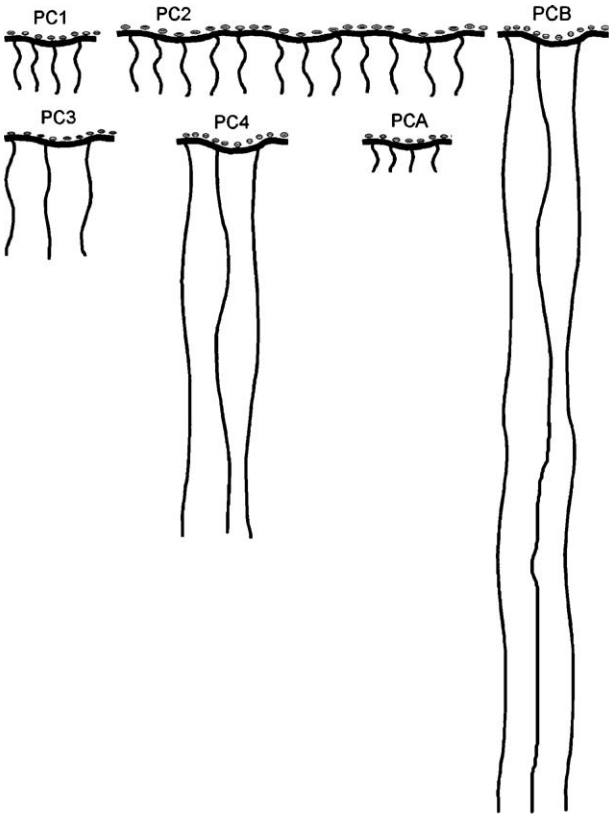

Fig. 1. Schematic illustration of the molecular structure comb-type copolymers with a negatively charged polycarboxylate backbone with grafted polyethylene-oxide side chains of different length.

coverage where the polymer PC 1 was added at a lower dosage; 0.41, 0.98, 2.00 and 4.00 mg polymer/g powder, respectively.

The polymer-containing suspensions were transferred into a polyallomer tube with dimension ø25 mm and length 89 mm. The bottom of the tubes had been made flat with an epoxy/lead ball mix, to minimise the radial stress gradient on the suspension and the resulting particle cake. The suspensions were centrifuged in a Mistral 2000 Small Capacity Bench centrifuge at 400 rpm for approximately 3 h. The distance from the rotational centre to the bottom of the tube was 160 mm. The centrifugation was terminated when the consolidation process had reached steady state, as determined from the variation in the cake height during centrifugation. The consolidation cake was cut into slices of a thickness of 2–3 mm following a modification of the procedure described by Meeten [20]. The water content, and thus the solids volume fraction of the slices (henceforth known as volume fraction), were determined by measuring the weight loss after drying at 105 °C. All experiments were repeated between 2 and 4 times and showed a variation in the volume fraction between 1% and 5% with a mean of 2%.

2.2.2. Particle size measurements

Particle size distributions of the remaining supernatant solutions were determined by light scattering using a Malvern Mastersizer 2000, Model APA2000 where particles between 20 nm and 2000 μm can be measured with an accuracy of ±1%.

3. Results and discussion

The rheological properties of a suspension are normally investigated by subjecting the system to a shear field. This can be done in several modes and give information about e.g. the steady shear viscosity as a function of shear rate or the shear yield stress. The yield stress is a very important parameter that is of profound importance for the flow properties of cementitious systems [21,22]. Concentrated suspensions can develop a yield stress when the particles are flocculated resulting in the formation of a continuous particle network, which can support a stress up to a critical value, the yield stress. Weakly flocculated suspensions with relatively coarse particles, typical for cementitious systems with added comb-type superplasticizers, are very difficult to characterise using shear rheology as the particle gels are very fragile and unstable. Preliminary work on the MgO suspensions showed that it was not possible to obtain a reliable measure of the shear yield stress when the comb-type superplasticizers had been added. However, it is also possible to determine the yield stress of a particle network that is subjected to a compressive stress gradient [22,23]. The compressive yield stress is typically two orders of magnitude greater than the shear yield stress and thus more sensitive to small variations in the degree of flocculation also in weakly flocculated systems [23,24].

Fig. 2 illustrates how the compressive yield properties can be determined by a simple centrifugation experiment. The centrifugal acceleration infers a force to the particles that results in a settling or consolidation of the particle network. The consolidation proceeds until the stress gradient that is developed in the particle network is balanced by the strength of the particle network. When consolidation has reached steady state, the stress on the particle network must be balanced; hence we can assume that the compressive yield stress, P_y, equals the applied stress at all levels and positions in the particle network. Determining the solids volume fraction profile of the centrifuged cakes thus gives information on the compressibility and strength of the particle networks as the stress on the particle network increases towards the bottom of the cake. Sedimentation experiments, although under normal gravity, have in fact been used not only to study early hydration kinetics of cement but also to infer the dispersing character of lignosulfonate type superplasticizers in cement suspensions [25].

Table 2
Information on the architecture of the comb-type polymers and maximum adsorbed amount at full surface coverage (from [15,16])

Polymer	Average molar mass, M_w [g/mol]	PMA backbone length, M_w [g/mol]	PEO side chain length, M_w [g/mol]	Adsorption on MgO [mg/g]
PC 1	23,000	6200	1000	1.29
PC 2	113,000	30,000	1000	1.32
PC 3	25,000	6100	2000	1.1
PC 4	61,000	7100	5000	1.08
PC A	35,000	9000	550	n.a.
PC B	45,000	7300	10,000	n.a.

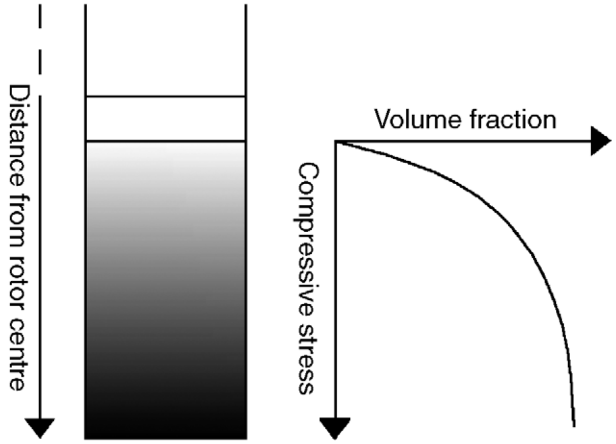

Fig. 2. Schematic illustration of a consolidated particle network with the associated compressive stress curve. The volume fraction of the centrifuged cake increase towards the bottom of the tube as the compressive stress increases with distance from the rotor centre and with the accumulated weight of the particle network.

3.1. Compressive yield behaviour at full surface coverage

Fig. 3 shows that the addition of comb-type superplasticizers to the MgO suspensions has a significant effect on the steady-state volume fraction profiles at a centrifugal speed of 400 rpm. All the suspensions displayed a compressible behaviour with an increasing volume fraction towards the bottom of the centrifuge tube (increasing distance from the rotor centre). This behaviour is typical for flocculated particle networks since a fully stable suspension is expected to display an essentially incompressible consolidation behaviour [26,27]. The MgO suspension without addition of any superplasticizer forms a particle network that attains a low volume fraction in the applied centrifugal force field (Fig. 3). This implies that the compressive yield stress is high and that the maximum stress that is applied at the bottom of the cake at a rotational speed of 400 rpm (approximately 6 kPa) only consolidates the MgO particle network to a volume fraction of $\Phi \approx 0.36$. Additions of superplasticizers result in an increase of the volume fraction at the bottom of the tubes, $\Phi \approx 0.43$–0.50, which shows that adsorption of the comb-type superplasticizers significantly reduces the compressive yield stress of these particle networks.

Centrifugation of the reference suspension without polymer addition resulted in the formation of a clear supernatant above the consolidated particle cake. This is a typical behaviour for a strongly flocculated suspension where all particles flocculate and are incorporated into the particle network. The addition of superplasticizers yielded a “milky” supernatant, containing small concentrations of very fine particles. Fig. 4 shows one example of the particle size distribution in the “milky” supernatant with a mean diameter of 150 nm. Comparative measurements with other comb copolymers added yielded a similar behaviour and particle size in the “milky” phase. This suggests that at least a fraction of the MgO particles is colloidally stabilised by the addition of the superplasticizers and thus is not incorporated into the consolidated particle network.

The consolidation study at full surface coverage indicates that the volume fraction and thus also the compressive yield stress depend on the molecular structure of the comb-type superplasticizers. Fig. 5 shows that the volume fraction obtained at the bottom of the tubes increases with the molecular weight of the grafted ethylene oxide side chains and approaches asymptotically a maximum value. This suggests that the length of the grafted side chains may control the consolidation behaviour of the particle network.

We have made an attempt to estimate the thickness of the adsorbed polymers at the surface of the MgO particles and rationalize how the polymers control the degree of flocculation. Recent direct force studies by Kauppi et al. [12] on commercially available comb-type superplasticizers suggest that the grafted side chain are coiled rather than stretched. Scaling theory predicts that there is a transition between the two modes that depends on the distance between the chains [28]. The coiled chains in the so-called mushroom conformation are predicted to

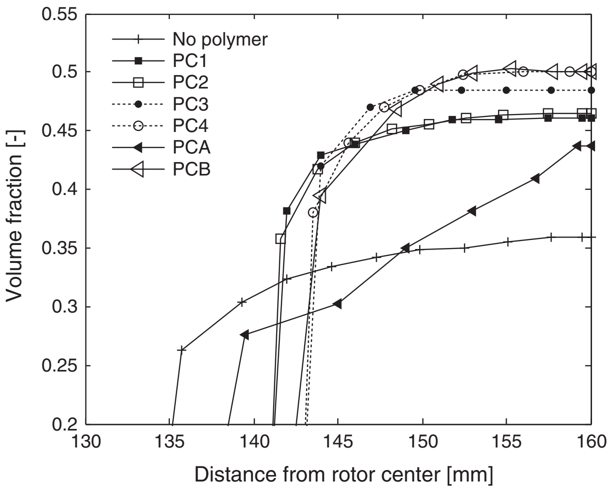

Fig. 3. Volume fraction profiles at steady state for MgO suspensions with different comb-type superplasticizers added. The suspensions were centrifuged at 400 rpm for 3 h.

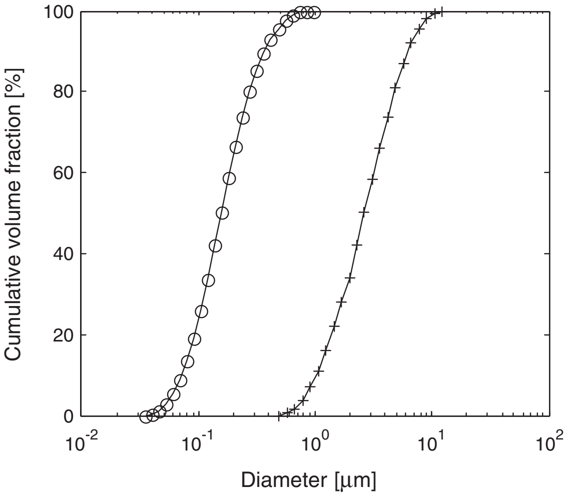

Fig. 4. Particle size distribution of the MgO suspension (+) and the supernatant (o) that remains when a suspension containing the comb copolymer PC1 has been centrifuged at 400 rpm for 3 h.

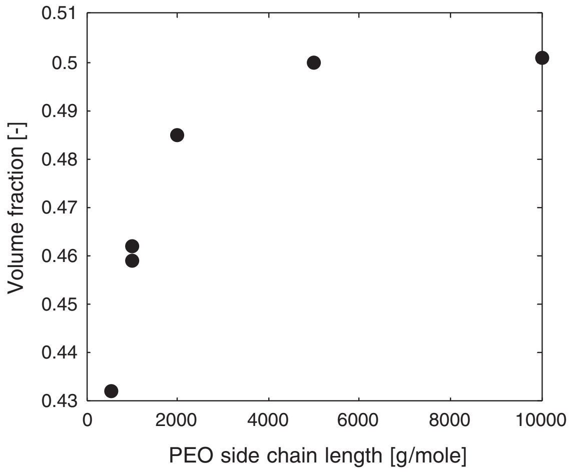

Fig. 5. The highest attained volume fraction after centrifugation at 400 rpm, as a function of the molecular weight, of the polyethylene oxide side chains on the superplasticizers.

become stretched and transfer into the so-called brush conformation when the average spacing between chains is less than twice their hydrodynamic radius.

The adsorption data given by Perche [16] on PC 1, 2 and 4 can be used to calculate the average area available on the surface of MgO for each PEO side chain at full surface coverage. The average separation distance D between the PEO side chains can be obtained with a simple calculation. Comparison with the estimated radius of gyration of PEO shows that the average separation distance is close to the radius of gyration but sufficiently large to support the use of the mushroom approximation in the estimation of the adsorbed layer thickness.

The layer thickness, δ, or the radius of gyration, R_F, of the adsorbed comb-type superplasticizers layer can thus be estimated from a simple expression for a mushroom conformation of the PEO side chains:

$$\delta = R_F = L_{PEO}(P)^{3/5} \tag{1}$$

Where L_{PEO} is the length of the ethylene oxide [$-CH_2-CH_2-O-$] segment (0.359 nm) and P is the number of segments in the chain.

Fig. 6 shows that the maximum volume fraction of the consolidated particle networks scales with the inverse of the estimated layer thickness. The simple relation clearly corroborates the importance of the grafted PEO-side chains in imparting a steric repulsion that controls the consolidation of the particle network. The inverse scaling could also be used in future work and assist in the design of optimal architectures of new types of superplasticizers.

It should be noted that the maximum volume fraction that we report is attained at the applied rotational speed, 400 rpm. Experiments were also carried out at higher speeds (3000 and 10,000 rpm) but at these speeds, all cakes, irrespective of polymer addition, consolidated to identical heights. At 3000 rpm, the maximum obtained volume fraction was 0.51 while at 10,000 rpm it was 0.54. Because of this, the maximum volume fraction obtained in the 400 rpm experiments is not the actual maximum obtainable volume fraction, ϕ_m, but the maximum obtainable volume fraction at these conditions.

The maximum volume fraction to which a particle network can pack is to a significant extent determined by geometrical factors, i.e. the shape and size distribution of the particles. The common volume fraction of 0.51 to which the particle networks consolidate to when the rotational speed is 3000 rpm is close to the maximum volume fraction that can be attained at 400 rpm when the layer thickness and thus the steric repulsion are large. This suggests that this volume fraction should be close to the maximum volume fraction. Hence, the MgO powder used in this study appears to have a relatively low maximum volume fraction of 0.51, which can probably mainly be related to the non-spherical shape. The slight increase in the measured volume fraction at even higher rotation rate (10,000 rpm) may be related to compression and deformation of the hydrated surface layer of the powders and should thus not be a representative of the geometrical packing of the non-deformed powder.

3.2. Compressive yield behaviour at sub-monolayer coverage

Superplasticizers are commonly added to cementitious systems at very low dosages, much below the amounts needed for full surface coverage. Fig. 7 shows how the consolidation behaviour varies with the amount of added PC 1 comb-type superplasticizer. We find that all the suspensions display a compressible behaviour with an increasing volume fraction towards the bottom of the centrifuge tube (increasing distance from the rotor centre). Increasing the addition of PC 1 results in an increase in the volume fraction at the bottom of the tubes. This suggests that an increase in the surface coverage reduces the compressive yield stress.

The relation between the maximum attained volume fraction at 400 rpm and the added amount of the superplasticizer PC 1 (Fig. 8) suggests a linear behaviour between dosage and volume fraction at low dosage. It is interesting to relate this observation to the previous adsorption studies by

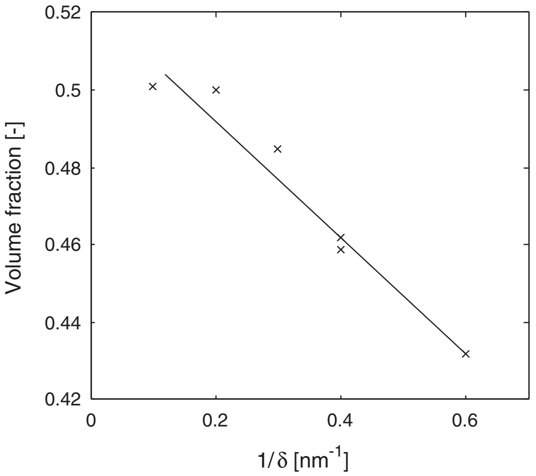

Fig. 6. The highest attained volume fraction after centrifugation at 400 rpm, as a function of the inverse of the estimated adsorbed layer thickness, $1/\delta$.

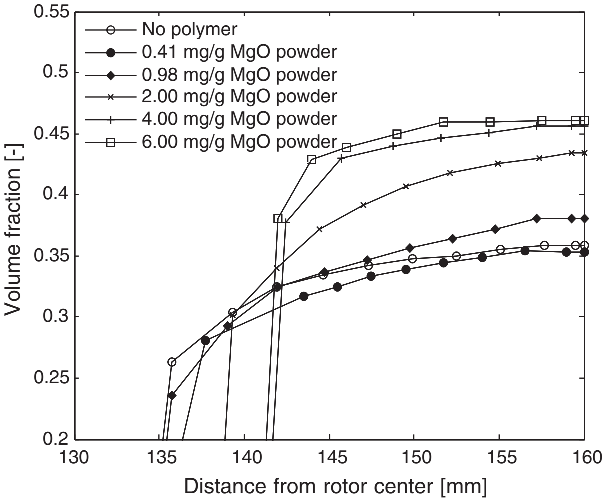

Fig. 7. Volume fraction profiles at steady state for MgO suspensions that have been centrifuged at 400 rpm for 3 h with various amounts of the superplasticizer PC 1 added.

Perche [16] (reproduced in Fig. 9), where a linear relation between dosage and adsorbed amount in the low surface coverage region is clearly shown. This linear relation between dosage and surface coverage has also been confirmed by zeta-potential measurements [17]. Hence, based on the assumption that there is a linear relation between dosage and adsorbed amount for PC1 on MgO in YS electrolyte, the data in Fig. 8 suggest that there should also be a linear relation between the attained volume fraction in centrifugal consolidation and the surface coverage at low surface coverage. At higher dosages, the situation is more delicate and a simple linear relation is not expected to be valid.

The continuous increase of the maximum attained volume fraction with dosage (or surface coverage) of PC1 that asymptotically approaches the volume fraction attained at full surface coverage also suggests that sub-monolayer coverage relates to a thinner "efficient" layer thickness compared to full surface coverage. As was shown in the previous section, it is clear that the layer thickness has a profound influence on the yield stress of the particle suspensions and from a technical perspective it is of interest in future studies to identify how the polymer structure can be optimized to yield a relatively large "efficient" layer thickness also at relatively low surface coverage.

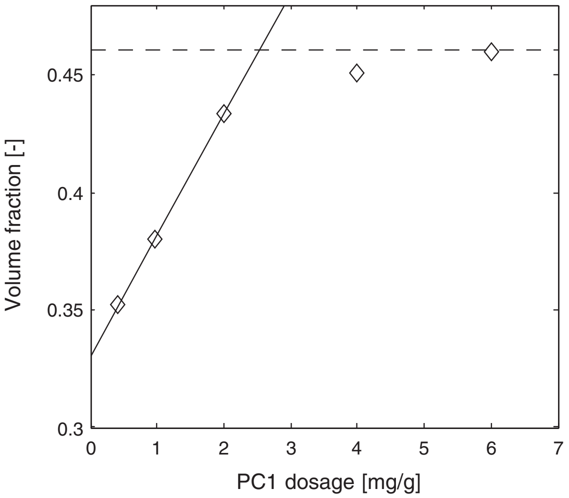

Fig. 8. Volume fraction at the bottom of the particle networks centrifuged at 400 rpm as a function of the added amount of the PC 1 superplasticizer. The linear relation between addition of polymer and volume fraction at low dosage is indicated by the full line and the maximum volume fraction at full surface coverage is indicated by the broken line.

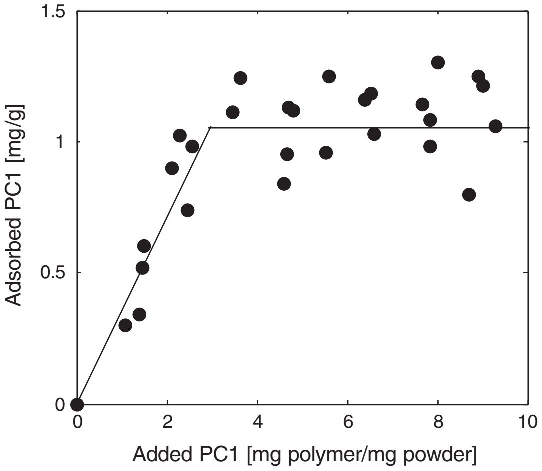

Fig. 9. Adsorption isotherm of PC1 in aqueous media at pH 12. From [16].

3.3. Scaling relation between consolidation behaviour and the inter-particle bond strength

The centrifugal consolidation results show that it is the thickness of the adsorbed polymer layer that plays a decisive role in controlling the rheological properties. In this section we outline a scaling approach which links the consolidation behaviour of the polymer-coated MgO particle networks, to the magnitude of the inter-particle forces.

The compressive yield stress of a particle network, P_y can be written as a product of a volume fraction function $f(\phi)$ and maximum attractive inter-particle force F_{max}:

$$P_y \approx f(\phi) F_{max} \tag{2}$$

In our experiments, we consolidate MgO suspensions containing various superplasticizers and measure the volume fraction profile. It is possible to estimate the applied stress by an integration procedure and thus obtain an estimate of how the volume fraction relates to P_y. Unfortunately, the small height of the consolidated cakes and the relatively small number of slices that the cake can be divided into mean that we only obtain an accurate estimate of P_y at the bottom of the tube. Hence, it is difficult to determine the yield stress dependence on volume fraction with sufficient accuracy. However, the use of the same amount of MgO powder in all the experiments means that the values of P_y are essentially identical at the bottom of the centrifuged particle networks for all samples, within

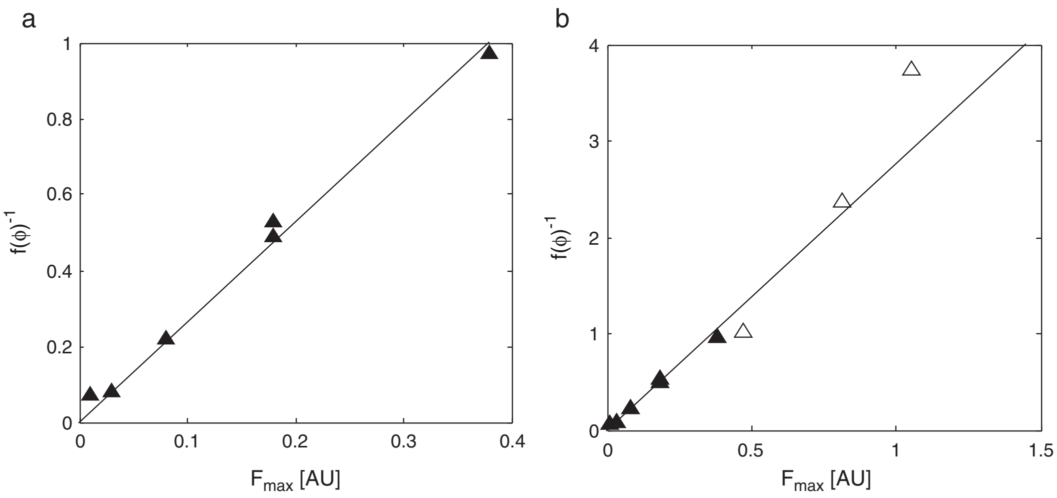

Fig. 10. The inverse of the assumed volume fraction function $f(\phi) \approx \frac{\phi^3}{\phi_{\max}-\phi}$ versus the estimated maximum attractive inter-particle force, $F_{\max}$. The points relate to the values for highest attained volume fraction after centrifugation at 400 rpm, and the $F_{\max}$ in arbitrary units calculated from the estimated layer thickness of the specific superplasticizer. Filled points relate to the systems at full surface coverage and the open triangles to the systems at sub-monolayer coverage of the superplasticizer PC 1.

experimental error. Hence, under the condition of constant P_y, it is possible to obtain a scaling between $F_{\max}$ and $f(\phi)$,

$$F_{\max} \propto 1/f(\phi) \tag{3}$$

which allows us to investigate in a quantitative manner how the layer thickness of the adsorbed superplasticizers controls the inter-particle forces and thus the consolidation behaviour.

The total inter-particle force between two particles consists of a summation of several contributions, e.g. the van der Waals force, the double layer force and the polymer-induced steric force.

The van der Waals force between two particles of equal radius a, and material ($_1$) acting across a medium ($_2$) can be approximated by [29,30]:

$$F_{\text{vdW}} \approx -A_{12} \cdot f_{\text{retardation}} \cdot \frac{\mathrm{d}H}{\mathrm{d}h} \tag{4}$$

where A_{12} is the Hamaker constant (see [31]), $f_{\text{retardation}}$ is a retardation factor that incorporates the retardation of the dipole interaction over large distances [32], H is a geometrical factor dependant on the shape of the interacting particles (see [27]) and h is the separation distance.

This relation simplifies to

$$F_{\text{vdW}} \approx -A_{12} \cdot \frac{a}{12h^2} \tag{5}$$

at close separation distances where the retardation is negligible.

Considering the very low surface charge and the high ionic strength that characterise these systems, it is possible to ignore the double layer contribution and simply estimate the maximum inter-particle bonding force, $F_{\max}$, from the van der Waals interaction at a separation distance twice the layer thickness, δ, of the adsorbed polymer [9]. Since we are only doing a scaling approach, it is sufficient to write:

$$F^*_{\max} \propto \delta^{-2} \tag{6}$$

The volume fraction dependence, $f(\phi)$, in Eq. (2) has received much attention and several models have been proposed [23,24,27]. The proposed models generally account for a divergence in P_y as the maximum volume fraction $\phi_{\max}$ is approached, e.g. by a term in the form of $(\phi_{\max}-\phi)^{-1}$. The inhomogeneous nature of the particle network and the associated density and fraction of the network through which the stress is transmitted, is usually included in the form of a power law dependence of P_y on the volume fraction, e.g. as ϕ^n (with $n \geq 2$). We have somewhat arbitrarily chosen a simple form of the volume fraction dependence [28]:

$$f(\phi) \approx \frac{\phi^3}{\phi_{\max}-\phi} \tag{7}$$

The inverse of this form of $f(\phi)$ with a maximum volume fraction $\phi_{\max}$, of 0.51 has been used to evaluate the scaling behaviour between the volume fraction that is attained at the bottom of the tubes centrifuged at 400 rpm against the inter-particle bond strength in Fig. 10. We find that Fig. 10a clearly establishes a linear scaling relation for the systems at full surface coverage that corroborates the importance of the range of the steric repulsion on the consolidation behaviour. We infer that similar relations, if not the same, must exist for shear rheology, although experimental issues discussed earlier may render their determination difficult. To our knowledge it is the first time that such a quantitative relation between superplasticizer structure and rheological properties of cement-like suspensions has been established.

It is tempting to extend the scaling approach to systems with incomplete surface coverage. The main problem in doing this consists in determining a relevant average maximum attractive inter-particle force. We propose a simple ad hoc approach which consists in determining the average inter-particle force by a

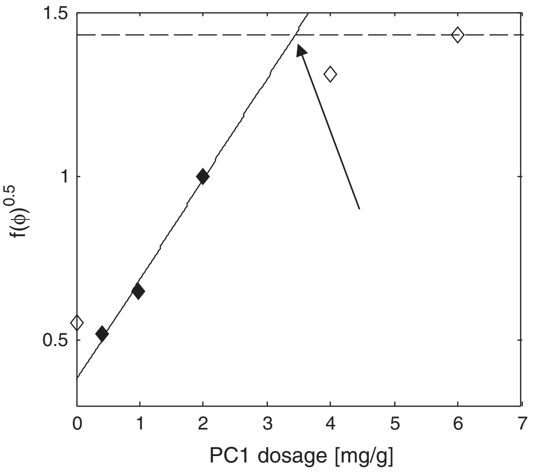

Fig. 11. Plot of $\sqrt{f(\phi)}$ versus dosage, *m*. The continuous line is the linear regression on the low dosage data argued for in the text. The discontinuous line is the value of $\sqrt{f(\phi)}$ for full surface coverage by PC 1. The interception of both lines indicated by the arrow indicates the point used to determine the "pseudo-saturation dosage" m^* that is used to estimate surface coverage in the low dosage range by m/m^* (see text).

weighted average of the layer thickness of the polymer covered surfaces:

$$F_{\max} \approx \left(\frac{\theta^2}{(\delta)^2} + \frac{8\theta(1-\theta)}{(\delta+\delta_0)^2} + \frac{(1-\theta)^2}{(\delta_0)^2} \right) \quad (8)$$

where θ is the surface coverage and δ_0 can be viewed as a solvation layer of half the minimum distance of approach for particles that are not coated by polymers.

To use Eq. (8), we need an estimation of the surface coverage. In the low dosage range, we can assume a linear relation between dosage and surface coverage [16]. However, the slope of the relation is not unity, indicating a constant partition between solution and surface. We therefore need to determine a "pseudo-saturation dosage", m^*, by which low dosages, *m*, can be normalised to obtain surface coverage m/m^*.

Eqs. (3) and (6) combine to give the scaling relation

$$\delta_\theta^* \approx \sqrt{f(\phi)} \quad (9)$$

where δ_θ^* denotes an average layer distance that would give a force equivalent to that in Eq. (8). This average layer thickness is a function of surface coverage θ and increases from δ_0 to δ as θ goes from zero to one.

As stated above, for low values of surface coverage, we expect θ to be proportional to dosage *m*. Therefore and according to Eq. (9), a plot of $\sqrt{f(\phi)}$ versus dosage is of the same nature as an equivalent plot versus surface coverage. In Fig. 11 we see that this relation is linear in the low surface coverage range. Extrapolating this linear trend to the point where $\sqrt{f(\phi)}$ corresponds to full surface saturation by PC1 can estimate the "pseudo-saturation dosage" as about 3.5 mg/g (arrow in Fig. 11). We now have the value m_0 which we can use to calculate surface coverage in the low dosage range by m/m^*.

The next step in our analysis of incomplete surface coverage is to estimate δ_0. We obtain this from the point where the force $F_{\max}$ at which $1/f(\phi=0.36)$ lies on the linear regression in Fig. 10a (0.36 is the volume fraction of the centrifuged MgO particle network that is obtained in the absence of polymer).

With the above, we get reasonable estimate of $F_{\max}$ also for sub-monolayer coverage, plotted in Fig. 10b. We find that the sub-monolayer data line up quite well with the extrapolation from data of complete surface coverage (filled symbols). However, it must be emphasized that further work is needed to determine the most appropriate way of determining the average inter-particle force. Furthermore, as surface coverage and thus also the attained volume fraction of the consolidated particle network decreases, the estimates of $1/f(\phi)$ will become increasingly sensitive to the exact form of $f(\phi)$ (Eq. (7)). Thus, these results at incomplete surface coverage must be viewed as demonstrating the potential extension of our scaling approach rather than a definitive word on the subject.

4. Summary and conclusions

The use of a compression rheology approach based on the analysis of centrifugally consolidated suspensions of MgO particles offers a novel tool to study and quantify the effect of the molecular structure of comb-type superplasticizers on the rheological properties. This simple experimental approach bypasses the issue of sedimentation and poor sensitivity that has been a common problem in steady-shear investigations.

We found that an increased length of the grafted ethylene oxide side chains of the adsorbed comb-type superplasticizers reduces the strength of the flocculated particle network and results in an increased volume fraction when the suspensions are consolidated at moderate rotational speeds. This is consistent with an increase in the range of the polymer-induced steric repulsion which reduces the degree of flocculation and thus also the compressive yield stress. Compression rheology studies at different dosage of a superplasticizer suggest that a reduction in the surface coverage increases the compressive yield stress. We showed that there is a linear relation between the attained volume fraction of the centrifuged suspensions and the surface coverage at low dosage.

We have also presented scaling relations for the influence of the length of the grafted ethylene oxide chains on the adsorbed layer thickness and the inter-particle forces. It was possible to establish a quantitative link between the molecular structure of the comb-type superplasticizers and the compression rheology behaviour of cement-like suspensions, based on established models for how the compressive yield stress should vary with volume fraction and the inter-particle forces. Suggestions for how the quantitative approach could be developed further were illustrated by an attempt to also treat systems at sub-monolayer coverage.

Acknowledgements

Dr. Irene Schober (Sika Technology AG) is specially thanked for providing the purified polycarboxylate polymers for this study.

The authors also acknowledge useful discussions with members of the EU project Superplast as well as financial support by the European commission for this project. Ane Kjeldsen was supported by The Danish Concrete Society, “Saxhofs Gavebrev” and SIKA Technology AG.

Annika Kauppi, Institute for Surface Chemistry (now at Sandvik Tooling, Sweden) is thanked for her help in providing materials and materials data.

References

[1] V.S. Ramachandran, V.M. Malhotra, C. Jolicoeur, N. Spiratos, Superplasticizers: Properties and Applications in Concrete, Ministry of public works and government services, Ottawa, Ontario, Canada, 1998.

[2] E. Sakai, M. Daimon, Dispersion mechanisms of alite stabilized by superplasticizers containing polyethylene oxide graft chains, in: V.M. Malhotra (Ed.), Proceedings of the 5th Canmet/ACI International Conference on Superplasticizers and Other Chemical Admixtures in Concrete, American Concrete Institute, Detroit, 1997, pp. 187–202, SP-173.

[3] H. Uchikawa, S. Hanehara, D. Sawaki, The role of steric repulsive force in the dispersion of cement particles in fresh paste prepared with organic admixtures, Cem. Concr. Res. 27 (1) (1997) 37–50.

[4] E. Sakai, M. Daimon, Mechanisms of superplastification, in: J.P. Skalny, S. Mindess (Eds.), Materials Science of Concrete, vol. IV, The American Ceramic Society, Westerville, OH, USA, 1995, pp. 91–111.

[5] K. Yoshioka, E. Sakai, M. Daimon, Role of steric hindrance in the performance of superplasticizers in concrete, J. Am. Ceram. Soc. (1997) 2667–2671.

[6] R.J. Flatt, Polymeric dispersants in concrete, in: V.A. Hackley, P. Somasundaran, J.A. Lewis (Eds.), Polymers in Particulate Systems: Properties and Applications, Marcel Dekker, New York, 2001, pp. 247–294.

[7] J.A. Lewis, H. Matsuyama, G. Kirby, S. Morissette, J.F. Young, Polyelectrolyte effects on the rheological properties of concentrated cement suspensions, J. Am. Ceram. Soc. 83 (8) (2000) 1905–1913.

[8] G.H. Kirby, J.A. Lewis, Comb polymer architecture effects on the rheological property evolution of concentrated cement suspensions, J. Am. Ceram. Soc. 87 (9) (2004) 1643–1652.

[9] R.J. Flatt, Towards a prediction of superplasticized concrete rheology, Mater. Struct. 27 (269) (2004) 289–300.

[10] K. Yamada, S. Hanehara, Interaction mechanism of cement and superplasticizers — the roles of polymer adsorption and ionic conditions of aqueous phase, Concr. Sci. Eng. 3 (2001) 135–145.

[11] I. Schober, U. Maeder, Compatibility of polycarboxylate superplasticizers with cement and cementitious blends, in: V.M. Malhotra (Ed.), Proc. 7th Canmet/ACI Int. Conf. on Superplasticizers and Other Chemical Admixtures in Concrete, American Concrete Institute, Framington Hills, 2003, pp. 453–468, SP-217.

[12] A. Kauppi, K.M. Andersson, L. Bergström, Probing the effect of superplasticizer adsorption on the surface forces using the colloidal probe AFM technique, Cem. Concr. Res. 35 (2005) 133–140.

[13] P.L. Hansen, J.A. Cohen, R. Podgornik, V.A. Parsegian, Osmotic properties of poly(ethylene glycols): quantitative features of brush and bulk scaling laws, Biophys. J. 84 (2003) 350–355.

[14] R.J. Flatt, P. Bowen, A. Siebold, Y.F. Houst, Cement model powders for superplasticizer properties studies, Proc. 11th ICCC, Durban, Tech book International, New Delhi, India, May 2003, pp. 676–685, (2).

[15] R.J. Flatt, Y.F. Houst, P. Bowen, H. Hofmann, J. Widmer, U. Sulser, U. Maeder, T.A. Bürge, Interaction of superplasticizers with model powders in a highly alkaline medium, in: V.M. Malhotra (Ed.), Fifth CANMET/ACI International Conference on Superplasticizers and Other Chemical Admixtures in Concrete (SP-173), ACI, Farmington Hill, Mi, USA, 1997, pp. 743–762.

[16] F. Perche, Adsorption de polycarboxylates et de lignosulfonates sur poudre modèle et ciments, PhD thesis # 3041, EPFL, Lausanne, Switzerland (downloadable at http://biblion.epfl.ch/EPFL/theses/2004/3041/EPFL_TH3041.pdf).

[17] F. Perche, Y. Houst, P. Bowen, H. Hofmann, Adsorption of lignosulfonates and polycarboxylates — depletion and electroacoustic methods, Proc. 7th CANMET/ACI International Conference on Superplasticizers and Other Chemical Admixtures in Concrete, Supplementary Papers, 2003, pp. 1–15, Berlin, Germany.

[18] A. Kauppi, P.F.G. Banfill, P. Bowen, L. Galmiche, Y.F. Houst, F. Lafuma, U. Mäder, F. Perche, B.G. Petersen, K. Reknes, I. Schober, A. Siebold, D. Swift, Improved superplasticizers for high performance concrete, Proc. 11th ICCC, Durban, Tech book International, New Delhi, India, May 2003, pp. 528–537.

[19] F. Perche, Y.F. Houst, P. Bowenand, H. Hofmann, Adsorption of lignosulfonates and polycarboxylates — depletion and electroacoustic methods, in: V.M. Malhotra (Ed.), 7th CANMET/ACI Int Conf on Superplasticizers and other Chemical Admixtures in Concrete, Supplementary Papers, 2003, pp. 1–15.

[20] G.H. Meeten, A dissection method for analyzing filter cakes, Chem. Eng. Sci. 48 (13) (1993) 2391–2398.

[21] P.F.G. Banfill, Rheology of Fresh Cement and Concrete: Proceedings of an International Conference, Liverpool 1990, Spon 1991.

[22] N. Pashias, D.V. Boger, J. Summers, D.J. Glenister, A fifty cent rheometer for yield stress measurement, J. Rheol. 40 (6) (1996) 1179–1189.

[23] R. Buscall, P.D.A. Mills, J.W. Goodwin, D.W. Lawson, Scaling behaviour of the rheology of aggregate networks formed from colloidal particles, J. Chem. Soc., Faraday Trans. 1 (84) (1988) 4249–4260.

[24] G.M. Channell, C.F. Zukoski, Shear and compressive rheology of aggregated alumina suspensions, AIChE J. (43) (1997) 1700–1708.

[25] J. Wheeler, S. Chatterji, The hindered setting of cement particles in freshly prepared Portland cement pastes: literature review-3, Indian Concr. J. (1973) 227–229.

[26] L. Bergström, Colloidal processing of ceramics, Handbook of Applied Surface and Colloidal Chemistry, John Wiley & Sons, Ltd, 2001.

[27] L. Bergström, C.H. Schilling, I.A. Aksay, Consolidation behavior of flocculated alumina suspensions, J. Am. Ceram. Soc. 75 (12) (1992) 3305–3314.

[28] R.J. Flatt, P. Bowen, Yodel: a yield stress model for suspensions, J. Am. Ceram. Soc. 89 (4) (2006) 1244–1256.

[29] R.J. Flatt, Dispersion forces in cement suspensions, Cem. Concr. Res. 34 (2004) 399–408.

[30] H. Pedersen, Particle interactions: an AFM study of colloidal systems. PhD-thesis. Technical University of Denmark, 1998.

[31] L. Bergström, Hamaker constants in inorganic materials, Adv. Colloid Interface Sci. (70) (1997) 125–169.

[32] W.B. Russel, D.A. Saville, W.E. Schowalter, Colloidal Dispersions, Cambridge University Press, 1989.